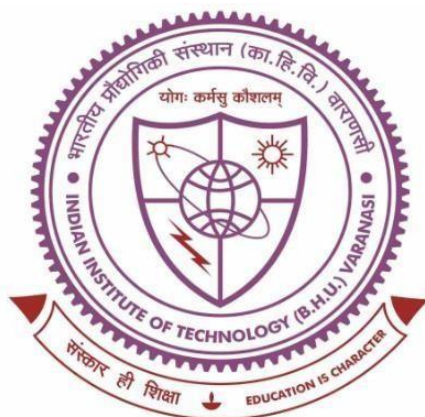


Multifunctional polymer nanocomposite thin films for tunable optoelectronics and flexible memory device applications



THESIS SUBMITTED IN PARTIAL FULFILLMENT FOR
THE AWARD OF DEGREE

Doctor of Philosophy

By

Shivam Awasthi

Department of Physics
Indian Institute of Technology
(Banaras Hindu University)
Varanasi-221005

Roll No. 18171510

2024



भारतीय
प्रौद्योगिकी
संस्थान
काशी हिन्दू विश्वविद्यालय



INDIAN
INSTITUTE OF
TECHNOLOGY
BANARAS HINDU UNIVERSITY

CERTIFICATE

It is certified that the work contained in the thesis titled “*Multifunctional polymer nanocomposite thin films for tunable optoelectronics and flexible memory device applications*” by *Shivam Awasthi* has been carried out under my supervision and that this work has not been submitted elsewhere for a degree.

It is further certified that the student has fulfilled all the requirements of the comprehensive examination, candidacy, and SOTA for the award of Ph.D. Degree.

Signature:

Supervisor

Signature:

Co-Supervisor

Dr. Anita Mohan
(Associate Professor)
Department of Physics
Indian Institute of Technology
(Banaras Hindu University)
Varanasi-221005 (UP)

Dr Kamalesh K Singh
(Professor)
Department of Metallurgical Engineering
Indian Institute of Technology
(Banaras Hindu University)
Varanasi-221005 (UP)



भारतीय
प्रौद्योगिकी
संस्थान
काशी हिन्दू विश्वविद्यालय



INDIAN
INSTITUTE OF
TECHNOLOGY
BANARAS HINDU UNIVERSITY

DECLARATION BY THE CANDIDATE

I, “*Shivam Awasthi*,” certify that the work embodied in this thesis is my own bonafide work and carried out by me under the supervision of “*Dr. Anita Mohan*” from “*January 2019*” to “*Jan 2024*” at the “*Department of Physics*,” Indian Institute of Technology (BHU), Varanasi. The matter embodied in this thesis has not been submitted for the award of any other degree/diploma. I declare that I have faithfully acknowledged and given credits to the research workers wherever their works have been cited in my work in this thesis. Furthermore, I also declare that I have not wilfully copied any other's work, paragraphs, text, data, results, etc., reported in journals, books, magazines, reports, dissertations, theses, etc., or available on websites and have not included them in this thesis and have not cited as my own work.

Date: 12/5/24

Place: IIT (BHU), Varanasi

Signature of the student

(Shivam Awasthi)

CERTIFICATE BY THE SUPERVISOR

It is certified that the above statement made by the student is correct to the best of my/our knowledge.

Supervisor

(Dr. Anita Mohan)

Signature of Head of Department

(Prof. Sandip Chatterjee)



भारतीय
प्रौद्योगिकी
संस्थान
काशी हिन्दू विश्वविद्यालय



INDIAN
INSTITUTE OF
TECHNOLOGY
BANARAS HINDU UNIVERSITY

COPYRIGHT TRANSFER CERTIFICATE

Title of the Thesis: Multifunctional polymer nanocomposite thin films for tunable optoelectronics and flexible memory device applications.

Name of the Student: Shivam Awasthi

Copyright Transfer

The undersigned hereby assigns to the Indian Institute of Technology (Banaras Hindu University) Varanasi all rights under copyright that may exist in and for the above thesis submitted for the award of the *“DOCTOR OF PHILOSOPHY”*.

Date: 11 May 2024

Place: IIT (BHU), Varanasi

Signature of the Student

(Shivam Awasthi)

Note: However, the author may reproduce or authorize others to reproduce material extracted verbatim from the thesis or derivative of the thesis for the author's personal use provided that the source and the Institute's copyright notice are indicated.

Acknowledgments

Completing this doctoral thesis has been a challenging yet fulfilling journey that would not have been possible without the support and contributions of numerous individuals and organizations. I am deeply grateful to all those who have helped me along the way.

First and foremost, I extend my heartfelt appreciation to my thesis supervisor, **Dr. Anita Mohan** and Co-Supervisor **Dr. Kamalesh K. Singh** whose guidance, patience, and expertise were instrumental in shaping this research. Your insightful feedback and unwavering encouragement have been invaluable throughout this process. I am also thankful to my thesis committee members **Dr. Sandip Chatterjee** and **Dr. R.K. Gautam** for their constructive criticism and valuable suggestions that significantly enhanced the quality of this work. I am thankful to my research collaborator **Dr. Bhola Nath Pal** for his excellent guidance during the course of the research. His expertise and technical suggestions helped me produce high-impact research works in the field. I also want to thank **Dr. Avanish Singh Parmar**, **Dr. P.C. Pandey** and **Dr. Chandan Upadhyay** for providing various synthesis and characterization facilities.

I extend my gratitude to my labmates and juniors Bhimraj Singh, Vikash Gupta, and Subarna Pramanik for being a significant part of my research. I owe a debt of gratitude to my colleagues, batchmates and friends who provided support and encouragement during this endeavor. A special thanks to Shubham, Monia, Kartika, Nidhi, Samiksha, Pawan, Kaustub, Anuvrat, Harsh, Ashish, Shweta, Neha, Aakanksha, Saurav, Sachin, and Santosh for being my constant companions throughout this journey. I convey my gratitude to all my teachers throughout my academic career for preparing me to walk through this long journey.

I am indebted to my family for their unconditional love, patience, and encouragement throughout my academic journey. Their unwavering belief in me has been a constant source of motivation. I express my heartfelt gratitude to my father, **Mr. Rajeev Kumar Awasthi** and mother, **Mrs. Archana Awasthi**. I also want to thank my sister Shweta Tripathi, brother-in-law Sachin Tripathi, my dear nephew and niece, Arush and Yashika and my beloved cousins Shrishti, Devansh and Apoorv. I also want to give a special mention to my very close friends

Tushar and Jigyasa who were always there by my side through thick and thin. This endeavour would have never been possible without the love and support of these people.

I am also thankful to all the technical, non-teaching as well as office staff of the Department of Physics, IIT (BHU) Varanasi for their assistance when required. Last but not least, I wish to thank all my friends and the persons whose names have not been included on this piece of paper for extending their cooperation directly or indirectly. I sincerely thank IIT BHU for providing me with the fellowship, training, a wonderful learning experience, and a chance to collaborate with people with great expertise in the field. I warmly thank the CIFIC, IIT (BHU) instrumentation facility for providing excellent research infrastructure.

Thank you to everyone who contributed to this work in various ways. Your support has been invaluable.

Sincerely

Shivam Awasthi

Table of Contents

CERTIFICATE	i
DECLARATION BY THE CANDIDATE	iii
COPYRIGHT TRANSFER CERTIFICATE	v
Acknowledgments	vii
Table of Contents	ix
Preface	19
Chapter 1 Introduction	25
1.1 Introduction to Functional Nanostructures	27
1.1.1 Metal and Metal Oxide Nanostructures	28
1.1.2 Functional Carbon-Based Nanostructures	30
1.1.3 Functional 2D Nanostructures	33
1.1.4 Functional Nanoscale Heterostructures	35
1.2 Introduction to nanocomposites	37
1.2.1 Types of Nanocomposites	38
1.2.2 Exploiting multifunctionality in nanocomposite material design	46
1.2.3 Synthesis methods of polymer nanocomposites	48
1.2.4 Applications of Polymer matrix nanocomposites	54
1.2.4.1 Aerospace:	54
1.2.4.2 Electronics:	55
1.2.4.3 Biomedical:	57
1.2.4.4 Environment:	58
1.2.4.5 Energy:	60
1.2.4.6 Optics & Photonics:	61
1.3 Research Background	63
1.4 Fundamental concepts pertaining to research	70
1.4.1 Self-Assembly of Nanoparticles	70
1.4.2 Oriented Attachment Crystal Growth	72
1.4.3 Zeta Potential and Colloidal Stability	75
1.4.4 Quantum Confinement in Semiconductors	77
1.4.5 Resistive Switching Phenomenon in Memory Devices	79
1.4.6 Conducting Filament Formation Mechanisms	81
1.5 Motivation behind the work	83
Chapter 2 Experimental Details: Instrumentation & Methodology	87

2.1 Synthesis Techniques	89
2.1.1 Sol-Gel Reflux Method	89
2.1.2 Modified Hummers Method.....	90
2.1.3 Solvothermal Method	92
2.1.4 Solution-Processed Spin Coating.....	94
2.2 Characterization & Measurement methods	95
2.2.1 X-ray diffraction	96
2.2.2 Transmission Electron Microscopy (TEM) and Selected Area Electron Diffraction	98
2.2.3 Field-Emission Scanning Electron Microscopy (FESEM) & Energy-Dispersive X-ray Spectroscopy (EDX).....	100
2.2.4 Atomic Force Microscopy (AFM).....	102
2.2.5 UV-Vis spectroscopy	104
2.2.6 Fourier-transform Infrared (FTIR) spectroscopy	106
2.2.7 Raman spectroscopy	107
2.2.8 Photoluminescence spectroscopy	109
2.2.9 Dynamic Light Scattering (DLS) and Zeta Potential analysis	111
2.2.10 X-ray Photoelectron Spectroscopy (XPS)	112
2.2.11 Thermal evaporation vacuum chamber.....	114
2.2.12 Semiconductor Parameter Analyzer	116
Chapter 3 Biomimetic self-assembly of colloidal ZnO Quantum Dots	119
3.1 Synthesis methodology.....	121
3.2 Oriented Attachment (OA) growth process.....	121
3.3 Experimental methods.....	124
3.4 Results & Discussion.....	124
3.4.1 Morphology and Self-assembly.....	124
3.4.2 Crystallographic studies	128
3.4.3 Polydispersity, Surface potential and Colloidal stability.....	129
3.4.4 Quantum Confinement in colloidal ZnO nanoclusters	132
3.4.5 Interfacial defect induced PL emission	134
3.5 Conclusion	136
Chapter 4 Interface engineered polymer nanocomposite thin films	137
4.1 Synthesis methodology.....	139
4.1.1 Materials	139
4.1.2 Fabrication of ZnO/PMMA hybrid thin films.....	139
4.2 Experimental methods.....	140

4.3 Results & Discussion.....	140
4.3.1 Microstructural Surface and Interfacial studies.....	140
4.3.2 Topography and surface roughness measurements.....	146
4.3.3 Surface and Interfacial Chemistry (XPS).....	149
4.3.4 Optoelectronic characteristics of nanocomposite thin films	151
4.4 Conclusion	154
Chapter 5 Structural, Chemical, and Optical properties of FLGO and rGO/ZnO.....	155
5.1 Synthesis methodology.....	157
5.2 Experimental methods.....	157
5.3 Results & Discussion.....	159
5.3.1 Structural analysis	159
5.3.2 Morphological analysis.....	161
5.3.3 Chemical analysis.....	163
5.3.4 Optical analysis	165
5.4 Conclusion	168
Chapter 6 Fabrication and electrical characterization of flexible resistive memory devices.....	169
6.1 Device Fabrication	171
6.2 Electrical characterization of devices.....	172
6.3 Results & Discussion.....	173
6.3.1 Electrical characterization	173
6.3.2 Endurance and Retention characteristics.....	176
6.3.3 Flexibility study.....	177
6.3.4 Band-gap modelling and carrier mechanism	180
6.3.5 Conduction Mechanism.....	182
6.3.6 Electrical and flexibility performance compared to recently reported PNC devices	184
6.4 Conclusion	185
Chapter 7 Summary and Future Scope.....	187
References.....	195
Publications.....	219
Conferences/Symposiums attended.....	221

List of Figures and Tables

- Fig 1.1: Key applications of Metal Oxide Nanoparticles
- Fig 1.2: Schematic of different morphologies of Carbon based nanostructures
- Fig 1.3: Schematic of commonly utilized 2D nanomaterials and their atomic structure
- Fig 1.4: Schematic of various kinds of hybrid nano-heterostructures
- Fig 1.5 Schematic of CNT reinforced Copper matrix Nanocomposites
- Fig 1.6 Schematic of expanded Graphite reinforced Ceramic matrix nanocomposites
- Fig 1.7 Schematic of Graphene nanoplatelet reinforced Polymer matrix nanocomposites
- Fig 1.8: Schematic of solution mixing method for synthesizing polymer nanocomposites
- Fig 1.9: Schematic of melt mixing method for synthesizing polymer nanocomposites
- Fig 1.10: Schematic of in-situ polymerization method for synthesizing polymer nanocomposites
- Fig 1.11: Schematic of electrospinning method for synthesizing polymer nanocomposites
- Fig 1.12: Schematic of sol-gel method for synthesizing polymer nanocomposites
- Fig 1.13: Schematic of mesocrystal formation via non-classical crystallization process
- Fig 1.14: Schematic of the need for research in new memory technologies.
- Fig 1.15: Schematic of the materials exhibiting resistive switching phenomenon
- Fig 1.16: Schematic of template-assisted nanoparticle self-assembly
- Fig 1.17: Dynamics of oriented attachment crystal growth via in-situ TEM imaging
- Fig 1.18: Schematic of quantum confinement effects in semiconductor quantum dots
- Fig 1.19: Schematic of a two-terminal Resistive memory device
- Fig 2.1 Schematic of Sol-gel reflux setup
- Fig 2.2: Schematic of Modified Hummers Reaction
- Fig 2.3: Schematic of heterostructure synthesis via Solvothermal reaction
- Fig 2.4: Schematic of Spin-coating process for thin-film deposition
- Fig 2.5 Digital image of the XRD setup

Fig 2.6 Digital image of the HRTEM setup

Fig 2.7 Digital image of the FESEM setup

Fig 2.8 Digital image of the AFM setup

Fig 2.9 Digital image of the UV-Vis Spectrometer

Fig 2.10 Digital image of the Fourier Transform Infrared Spectrometer

Fig 2.11 Digital image of the Raman Spectroscope

Fig 2.12 Digital image of the Photoluminescence Spectrometer

Fig 2.13 Digital image of the DLS and Zeta Potential setup

Fig 2.14 Digital image of the X-Ray Photoelectron Spectroscope

Fig 2.15 a) Schematic of thermal evaporation technique for electrode deposition; b) Digital image of the thermal evaporator

Fig 2.16 Digital image of the Semiconductor Parameter Analyzer

Fig 3.1- Schematic description of ZnO nanocrystal surface modification and diethanolamine assisted self-assembly into ordered nanoclusters.

Fig 3.2- HR-TEM image of a single ZnO superstructure illustrating oriented attachment of crystal planes between neighboring Quantum dots.

Fig 3.3- TEM images of ZnO nanoclusters illustrating (a) Uniform and homogenous distribution of self-assembled structures at 100 nm resolution, (b) Porous morphology with individual QD's in 3-5 nm range at 50 nm resolution.

Fig 3.4- Histograms of (a) Size distribution of Quantum dots constituting a single nanocluster and (b) Size distribution of ZnO nanoclusters in the colloidal suspension

Fig 3.5- Top panel: (a) HRTEM image depicting highly aligned adjacent crystal planes with inset-a Fast Fourier transform of lattice planes, (b) Interplanar spacing of a nano-crystallite corresponding to $\langle 100 \rangle$ plane and (c) SAED pattern in reciprocal space

Fig 3.6- X-ray diffraction patterns of (a) Pure PMMA thin film and (b) 0.5 wt % PMMA/ZnO nanocomposite thin film on plasma treated polycrystalline Si wafers.

Fig 3.7- DLS measurements on colloidal ZnO QD ethanol suspension: (a) Correlation coefficient decay curve vs. time and (b) Intensity-wise particle size (hydrodynamic radius) distribution

Fig 3.8- (a) Zeta potential of surface-engineered colloidal ZnO QD suspension with a high positive peak value of 46.6 mV and (b) Digital photograph of ZnO suspension with high transparency after 6 months of storage depicting excellent colloidal stability.

Fig 3.9- Schematic of ZnO surface charge modification by diethanolamine depicting the particle surface, stern layer and potential at the surface of slipping plane (Zeta potential)

Fig 3.10- (a) UV-Vis absorbance data with $\lambda_{1/2}$ representation used in Meulenkamp method and (b) Tauc's plot depicting size-dependent blue shift in ZnO QD band gap.

Fig 3.11- PL emission spectra of ZnO nanocluster depicting oxygen vacancy and oxygen interstitial surface defect induced green and orange emission bands respectively.

Fig 4.1- (a) FE-SEM image showing the microstructure of PMMA surface & (b) Homogenously distributed ZnO nanoclusters in PMMA matrix (0.25 wt%) with absence of any agglomerates, (Inset-b) Thin PMMA layer covered surface of a porous self-assembled ZnO nanocluster.

Fig 4.2- (a,c) FE-SEM images of 2 wt% and 5 wt% nanocomposite thin films respectively.

(b,d) EDX spectra and corresponding elemental composition of 2 wt% and 5 wt% nanocomposite thin films respectively. (Unmarked peaks correspond to the ITO coated substrate)

Fig 4.3- Composite element map of 2 wt% ZnO/PMMA hybrid along with elemental composition of C,O,N and Zn.

Fig 4.4 : FESEM micrograph of 2 wt % ZnO/PMMA nanocomposite thin film. The white dots in the image represent the ZnO distribution (Element map fig 4.5-c)

Fig 4.5-a : Elemental distribution of C in Fig 4.4

Fig 4.5-b : Elemental distribution of O in Fig 4.4

Fig 4.5-c : Elemental distribution of Zn in Fig 4.4

Fig 4.5-d : Elemental distribution of N in Fig 4.4

Fig 4.6- Top panel: (a & d) Surface topography, (b & e) Phase images, (c & f) Surface roughness profiles of Pristine PMMA (P1) and PMMA/ ZnO nanocomposite (PZ-3) thin films respectively. Bottom panel: Three dimensional surface topographic profile of 0.5 wt% PMMA/ZnO nanocomposite thin film generated by Gwyddion software.

Fig 4.7- High resolution XPS spectra of 0.1 wt % PMMA/ZnO nanocomposite thin film in (a) C1s region with characteristic PMMA peaks, (b) Zn2p region depicting spin-orbit splitting in 2p levels, (c) O1s region with characteristic Zn-O peak and (d) N1s region indicating covalent bond between PMMA and DEA molecules on ZnO surface.

Fig 4.8- UV-Vis spectra of 2 wt % ZnO/PMMA hybrid with 85-90 % transparency in the visible region.

Fig 4.9- PL emission spectra of ZnO nanocluster and 2 wt% ZnO/PMMA hybrid depicting oxygen vacancy and oxygen interstitial surface defect induced green and orange emission bands respectively.

Fig 5.1: X-ray diffraction spectra of a) GO nanosheets and b) rGO_ZnO heterostructures.

Fig 5.2: HRTEM images of a) GO nanosheets and b) rGO_ZnO heterostructures with SAED crystal structure data in inset.

Fig 5.3: FESEM images of a) GO nanosheets and b) rGO_ZnO heterostructures. EDX spectra and elemental composition of c) GO nanosheets and d) rGO_ZnO heterostructures

Fig 5.4: AFM surface topography images of a) GO nanosheets and b) rGO_ZnO heterostructures.

Fig 5.5: Thickness/Height profile derived from AFM topography of a) GO nanosheets and b) rGO_ZnO heterostructures.

Fig 5.6: FTIR spectra of a) GO nanosheets and b) rGO_ZnO heterostructures in transmittance mode.

Fig 5.7: Raman spectra of a) GO nanosheets and b) rGO_ZnO heterostructures.

Fig 5.8: UV-Vis absorption spectra of a) GO nanosheets and b) rGO_ZnO heterostructures.

Fig 5.9: Tauc plot corresponding to UV-Vis absorption spectra of a) GO nanosheets and b) rGO_ZnO heterostructures.

Fig 5.10: Deconvoluted PL emission spectra of a) GO nanosheets and b) rGO_ZnO heterostructures.

Fig 6.1: Schematic of hierarchical architecture of hybrid heterostructure based flexible device

Fig 6.2: AFM picture in the scratched area of PNC film a) PMMA/rGO/ZnO film and c) PMMA/GO film. Line scan height profile of b) PMMA/rGO/ZnO film and, d) PMMA/GO film

Fig 6.3: I-V characteristics of a) M1 device and b) M2 device depicting bistable non-volatile memory operation.

Fig 6.4: Endurance cycle measurements of a) M1 device and b) M2 device

Fig 6.5: Current values in HRS and LRS after multiple switching cycles for a) M1 device and b) M2 device

Fig 6.6: Retention time measurements of high conductance state (HCS) and low conductance state (LCS) of a) M1 device and b) M2 device

Fig 6.7: I-V characteristics of M1 device under different bending radii.

Fig 6.8: a) Current values of M1 device in the HRS and LRS after multiple bending cycles, b) Current values of M1 device in the HRS and LRS under different bending radii and without bending.

Fig 6.9: Band-gap modelling of M1 device depicting the carrier mechanism; a) Energy band without bias, b) zoom view of PMMA/(rGO/ZnO NP)/PMMA, c) device under low negative bias, d) device under high negative bias, e) device under low positive bias, f) device under high positive bias.

Fig 6.10: I-V characteristics of M1 device in double logarithmic scale illuminating the conduction mechanism in both HRS and LRS.

List of Tables

Table 4.1- Advance surface roughness parameters computed for P1- Pristine PMMA film and PZ3- 0.5 wt% PMMA/ZnO nanocomposite film.

Table 6.1: Flexibility and electrical performance of this device in comparison to recently published literature.